

# Linear-time classical approximate optimization of cubic-lattice classical spin glasses

Adil A. Gangat<sup>1,2</sup>

<sup>1</sup>*Physics & Informatics Laboratories, NTT Research, Inc., Sunnyvale, CA 94085*

<sup>2</sup>*Division of Chemistry and Chemical Engineering, California Institute of Technology, Pasadena, CA 91125*

(Dated: February 14, 2025)

Computing low-energy configurations (i.e., approximate optimization) of classical spin glasses is of relevance to both condensed matter and combinatorial optimization. Recent theoretical work opens the possibility to make its time complexity with quantum annealing generically polynomial, and D-Wave experiments can now achieve approximate optimization of cubic-lattice classical Ising spin glasses with  $\sim 10^4$  spins. It is therefore timely to ask which short-range classical spin glasses are good candidates for demonstrating quantum advantage in the time complexity of heuristic approximate optimization. One intuition is to consider models with very rugged energy landscapes in configuration space. However, here we provide evidence that short-range classical spin glasses may be approximately optimized in linear time and space with a very simple deterministic tensor-network heuristic regardless of ruggedness. On the cubic lattice with up to  $50 \times 50 \times 50$  spins, we obtain energy errors of  $\lesssim 3\%$  for the  $\pm J$  model used in recent D-Wave experiments, and  $\lesssim 5\%$  for much more rugged planted-solution instances. For cubic-lattice-Ising reductions of unweighted Max-Cut on random 3-regular graphs with up to 300 vertices, we find energy errors of  $< 1\%$  and approximation ratios of about 72-88%. A theoretical implication of our algorithm is that only quantum algorithms with sublinear time complexity may have time-complexity quantum advantage for heuristic approximate optimization of classical spin glasses that have decaying correlations. These results inform the search for quantum advantage and suggest an efficient classical method for generating warm starts for other spin-glass optimization algorithms. Our algorithm is amenable to massive parallelization and may also allow for low-power, accelerated implementations with photonic matrix-multiplication hardware.

## I. INTRODUCTION

Classical, short-range spin-glass Hamiltonians have both fundamental and applied significance. One example is the classical Ising model on the simple cubic lattice, whose Hamiltonian is given by

$$H = \sum_{\langle i,j \rangle} J_{ij} \sigma_i \sigma_j, \quad (1)$$

where  $J_{ij} \in \mathbb{R}$ ,  $\sigma_i \in \{\pm 1\}$ ,  $i$  and  $j$  are lattice-site indices, and  $\langle \cdot \rangle$  denotes a restriction to nearest neighbors on the simple cubic lattice. When  $J_{ij}$  follows a random distribution (typically bimodal or Gaussian), this model is known as the classical Edwards-Anderson Ising model with zero field and is thought to capture the fundamental physics of spin-glass materials [1]. Yet, its low-temperature phase remains incompletely understood despite decades of effort [2]. On the applied side, computing the ground state of Eq. (1) is known to be NP-hard [3], and a more structured choice of  $J_{ij}$  allows it to encode problems in discrete combinatorial optimization [4]. Therefore, computing the low-energy solutions (i.e., approximate optimization) of Eq. (1) can be useful for both condensed matter physics and combinatorial optimization.

Recent developments in quantum annealing make the simple-cubic-lattice model of Eq. (1) particularly relevant to the issue of quantum advantage: On the experimental front, D-Wave and collaborators have recently demonstrated the approximate optimization of such a model with over 5,000 spins with pure quantum annealing [5] and over 11,000 spins with hybrid quantum annealing [6]. On the theoretical side, the recent work in Refs. [7, 8] presents the possibility of achieving generic polynomial time complexity for heuristic approximate optimization [9] of classical Ising spin glasses with quantum

annealing. Therefore, quantum advantage in the computational time complexity for heuristic approximate optimization of Eq. (1) may be possible in the near- to mid-term, but it is not clear for which instance classes of  $J_{ij}$ , if any; understanding where known classical algorithms are slow with this task can provide clues.

State-of-the-art Markov-Chain-Monte-Carlo algorithms are considered to be some of the best general classical heuristics for approximate and exact optimization of spin glass models. Consequently, (classical) computational hardness has become synonymous in the spin-glass literature with Monte-Carlo hardness (e.g., Ref. [10]). For this reason, Ref. [11] suggests that spin-glass models that display a steep increase in the autocorrelation time of parallel-tempering Monte Carlo as the temperature is lowered are good places to demonstrate quantum advantage. Also, Ref. [12] shows a time-complexity advantage of (error-corrected) quantum annealing over parallel tempering Monte Carlo (with isoenergetic cluster moves) for approximate optimization of a quasi-2D spin glass, and concludes this to be a demonstration of algorithmic quantum speedup. The hardness of certain spin glass instances for Monte-Carlo (and other) optimization algorithms that traverse the spin-configuration space is understood to be due to the rugged energy landscape (i.e., a plethora of local minima) that arises at low temperatures in that space. Even machine-learning enhancements of Monte Carlo methods have been shown to be ineffective at overcoming this source of computational hardness [13]. However, it is thought that quantum algorithms may be able to overcome this source of hardness via quantum tunneling [14–16].

It would seem, then, that one simply needs to find instances of Eq. (1) whose approximate optimization with the best Monte-Carlo algorithms is computationally hard (i.e., ex-

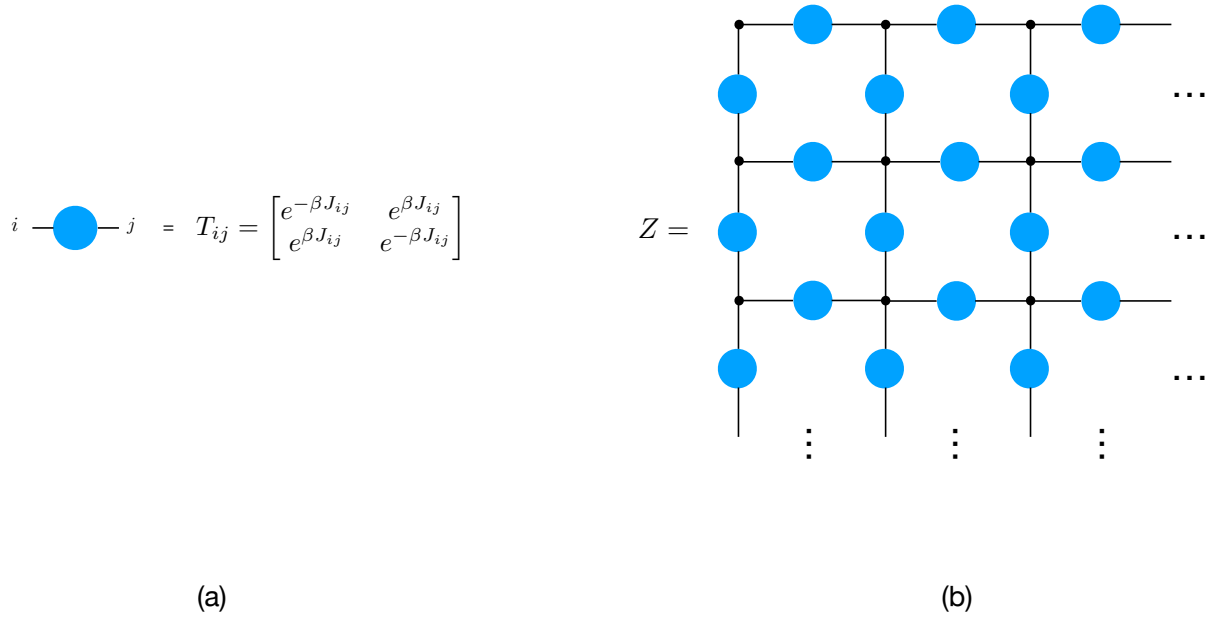


FIG. 1. (color online). (a) A large (blue) circle with two legs represents a two-index tensor of Boltzmann weights. The index dimension is equal to the number of possible classical single-spin configurations (in this case two, corresponding to Ising spins). (b) Tensor network representation of the partition function for a square-lattice classical Ising model. Small (black) circles denote the sites of spins. The joining of legs from different tensors represents a contraction of the tensors along a common (hyper)index. The contraction of the entire network yields the partition function.

hibits or at least hints at superpolynomial time complexity) in order to identify good candidates for demonstrating time-complexity quantum advantage in heuristic approximate optimization. However, Ref. [17] provides evidence that short-range rugged-energy-landscape spin glasses may be heuristically approximately optimized classically in quadratic time with approximate contractions of tensor networks, though the wall time for cubic lattices with that heuristic proves to be too large to be practical for large systems. Here we present a major advance over that result: We demonstrate a very simple deterministic tensor-network heuristic that is able to compute in linear time (and space) at least some (but not necessarily all) spin configurations that have energies within a few percent of the ground-state energy for the following three versions of Eq. (1): (1) the cubic-lattice  $\pm J$  model that is used in the D-Wave approximate optimization experiments in Refs. [5] and [6], (2) a planted-solution, cubic-lattice model whose hardness (i.e., time to exact optimization) for state-of-the-art Monte Carlo heuristics is orders of magnitude more than the  $\pm J$  model, and (3) a cubic-lattice model that encodes (unweighted) Max-Cut on random 3-regular graphs. Unlike the heuristic in Ref. [17], the present one is able to address very large cubic-lattice systems in a practical amount of time. We also provide an explanation for why this heuristic implies that *a quantum algorithm must have sublinear time complexity in order to have quantum advantage in the time complexity of heuristic approximate optimization of classical spin glasses that have correlations that decay with euclidean distance*, such as models (1) and (2) just mentioned.

The tensor-network algorithm presented here relies on a tensor-network representation of the partition function, and

is made possible through the following line of developments: First, the work in Refs. [18–21] presented ways of using tensor-network algorithms for *homogeneous* classical lattice models. This included a method of sampling from the Boltzmann distribution of homogeneous, two-dimensional classical spin lattices [21]. Then, Ref. [22] showed that the partition function of an *inhomogeneous* classical spin lattice may be exactly represented by the contraction of a network of tensors where the geometry of the network reflects that of the Hamiltonian’s interaction graph; while an exact contraction of the full network has an exponential cost, the contraction of the full network may be approximated, via truncated matrix decompositions, in polynomial time. Ref. [23] then, analogously to the work in Ref. [21] for homogenous systems, demonstrated how to use this idea to sample (via computation of conditional marginals) the low-temperature Boltzmann distribution of planar and quasi-planar spin glasses in polynomial time. Finally, Ref. [17] used a technically different type of approximate contraction from Ref. [23] to generate near-optimal solutions of spin glasses on periodic square and cubic lattices in quadratic time. In both of the latter two works, the time complexity is determined by the complexity of contracting the network and not the Monte-Carlo hardness (which is related to the ruggedness of the free-energy landscape in configuration space), and the heuristic is successful in generating near-optimal solutions for all tested problem instances. We note, however, that the data in Ref. [17] for cubic-lattice spin glasses only spans two sizes ( $4 \times 4 \times 4$  and  $6 \times 6 \times 6$ ) due to the high absolute time cost.

Compared to the approach in Ref. [17], here we present a more efficient way of using tensor-network representations

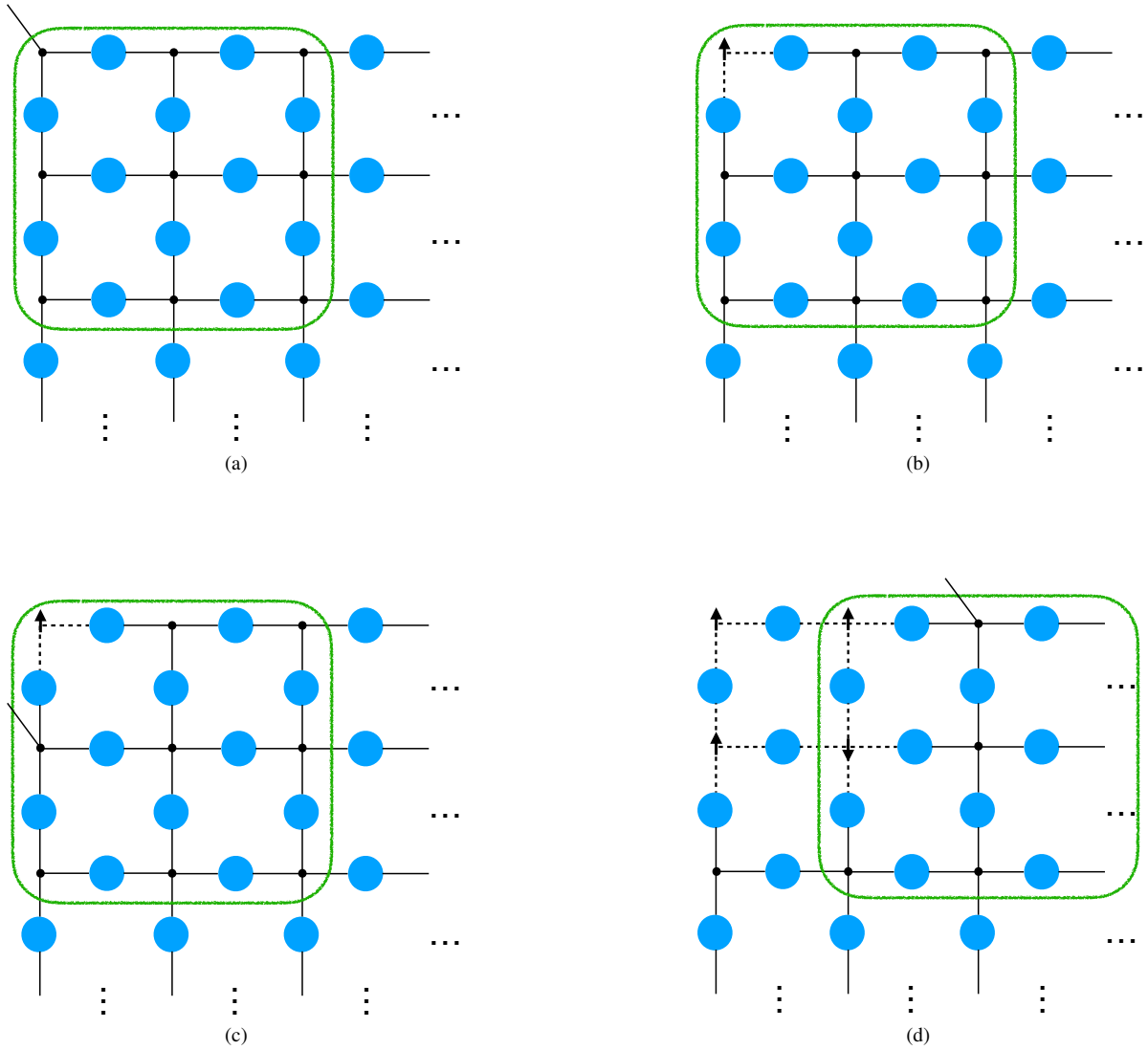


FIG. 2. (color online). Local energy minimization bootstrapping procedure. (a) Adding an open leg to a single black circle turns it into a kronecker delta function such that the contraction of the entire network yields a vector that is the (unnormalized) unconditional marginal for the corresponding spin. In the present algorithm, the approximation is made to compute the marginals by contracting only a local fragment, defined by the tensors within the fuzzy (green) rounded-square boundary (tensors with legs that cross the boundary are not included in the fragment). The spin is decimated by choosing its most probable configuration according to this approximate marginal. (b) The decimation is graphically denoted by legs with dashed lines and an up or down arrow (denoting  $+1$  or  $-1$ ). The decimation is internally accomplished by selecting the appropriate value of the corresponding index. (c) Adding an open leg to a different black circle after decimating previous spins yields the (unnormalized) marginal for the corresponding different spin. The marginal for this spin is conditional upon the configuration of the previously decimated spins that lie within the fragment. If  $\beta$  is sufficiently large, decimating spins in this manner results in an approximate local energy minimization. (d) Performing sequential decimations by overlapping the fragment with at least some of the previously decimated spins yields a bootstrapping of approximate local energy minimizations over the whole lattice. Using multiple fragments simultaneously (not shown) yields parallelization.

of classical, cubic-lattice spin-glass partition functions for approximate optimization. In Refs. [23] and [17], the amount of the network that is utilized to compute conditional marginals for single spins grows with the number of spins ( $N$ ) that are conditioned upon (though Ref. [17] always uses the full net-

work for simplicity). This leads to a time complexity for computing a total spin configuration that is quadratic in the total number of spins (an exponential complexity is avoided by making approximations via truncated matrix decompositions). The method in the present work instead has a *linear* time (and

memory) complexity for short-range classical spin glasses, and also eliminates the need for matrix decompositions. These improvements result in a dramatic speedup, and can be understood via a very simple intuition about short-range-correlated spin glasses: bootstrapping of approximate *local* energy minimization should lead to approximate *global* energy minimization. By “short-range-correlated” we mean that the couplings of the short-range Hamiltonian do not have long-range correlations, and by “bootstrapping” we mean requiring consistency between the spin configurations of the overlapping system fragments that are used for the local energy minimizations. Since the approximate local energy minimizations are done via *exact* contractions of tensor-network fragments of fixed size, bootstrapping them over the system requires no matrix decompositions and has  $\mathcal{O}(N)$  time complexity. While such a local optimization method will be biased against spin configurations with large-scale structures, such as droplets, it is intuitive that not all low-energy configurations will have such structures. We find that this method allows us to approximately optimize short-range-correlated cubic-lattice classical spin glasses that are orders of magnitude larger than those in Ref. [17]. Somewhat surprisingly, we also find the method to work well for cubic-lattice Hamiltonians that encode the long-range-correlated problem of unweighted Max-Cut on random 3-regular graphs.

The present heuristic shares the local-optimization spirit of the algorithm in Sec. III. of Ref. [24], but it is different in the following crucial ways: (1) the present algorithm aims at only *approximate* optimization instead of exact optimization, (2) the present algorithm has a guaranteed linear time complexity, and (3) the present algorithm consists almost purely of matrix multiplications (i.e., exact contractions of tensor networks).

Due to the ubiquity of matrix multiplication in computing, specialized photonic hardware for it, which seeks to improve both power consumption and speed over conventional processors, is under active development [25–28]. The present heuristic thereby serves, in principle, as the basis for a new type of specialized computing machine for obtaining near-optimal solutions of certain types of discrete combinatorial optimization problems.

In Section II we provide details of the heuristic algorithm. In Sections III A, III B, and III C we respectively present results for the  $\pm J$  model; the hardest instance class of the cubic-lattice tile-planted-solution model; and the cubic-lattice model that encodes (unweighted) Max-Cut on random 3-regular graphs. In Section IV we explain the implications of the algorithm for where quantum advantage may theoretically be found. We conclude in Section V with a summary and discussion.

## II. ALGORITHM

As explained in Refs. [17, 23, 29] both conditional and unconditional single-spin marginals for a classical spin glass in the canonical ensemble can be computed via the contraction of a tensor network wherein the indices of a given tensor correspond to single-spin configurations and the elements of the

tensor correspond to the Boltzmann weights of the joint configurations of the spins at the tensor’s legs (e.g., a two-index tensor contains the Boltzmann weights for the configurations of two spins); the geometry of the tensor network mirrors the geometry of the Hamiltonian’s interaction graph. The contraction of the network results in a multiplication of the local Boltzmann weights across the whole system that yields the (conditional or unconditional, depending on details of the network) marginal for the spin of interest. See Fig. 1 and Appendix A of Ref. [17] for further explanation. Computation of conditional single-spin marginals, and single-spin decimations according to those single-spin marginals, allows one to sample the Boltzmann distribution

$$p(\mathbf{s}) \sim \exp[-\beta H(\mathbf{s})], \quad (2)$$

where  $\mathbf{s}$  is a spin configuration vector for the entire system. For computing the exact ground state, exact contractions of the network are required with the inverse temperature  $\beta$  set to infinity. While infinite  $\beta$  is not numerically accessible, and exact contractions of the entire network are too costly for large systems, the intuition behind the heuristic in Ref. [17] is that *approximate* contractions of the entire tensor network with sufficiently large  $\beta$  should yield low-energy spin configurations. For further details we refer the reader to Ref. [17].

The algorithm in this work is a modification of the one in Ref. [17]: the marginal of a single spin is (approximately) computed by exactly contracting only a fragment of the network that is local to the spin of interest. Sequentially computing single-spin marginals with tensor-network fragments that overlap previously decimated spins results in a bootstrapping of approximate local energy minimization if  $\beta$  is sufficiently large (see Fig. 2 for an illustration on the square lattice). The intuition behind this approach is that if the Hamiltonian is not long-range correlated, then such a bootstrapping should also result in an approximate *global* energy minimization. Such an outcome would be consistent with the finding in Ref. [17] that approximate optimization can be successfully accomplished for short-range-correlated Hamiltonians with approximate contractions of the full tensor network that use only small bond dimensions. In this work we implement the new algorithm with the Python libraries `quimb` [30] and `cotengra` [31] on an Apple M2 Ultra CPU (16 performance and 8 efficiency cores) with 128 GB of RAM. We note that in two and higher dimensions this algorithm is straightforward to parallelize by using multiple fragments simultaneously, though we do not do so here.

## III. RESULTS

### A. cubic-lattice $\pm J$ model

This model is described by Eq. (1) with  $J_{ij}$  chosen from a uniform distribution over  $\{\pm 1\}$ . We use systems with dimensions  $L \times L \times L$  spins and periodic boundary conditions. To compute the relative energy error from the ground state, we use the value of the ground state energy density for the thermodynamic limit that is numerically estimated in Ref. [32].

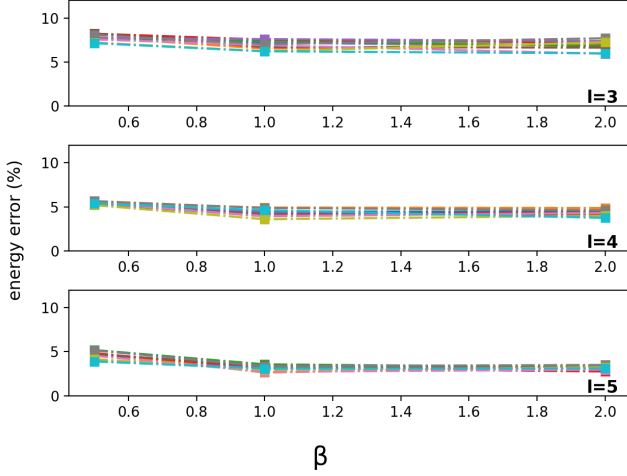


FIG. 3. (color online). Cubic-lattice  $\pm J$  model ( $20 \times 20 \times 20$  spins, periodic boundaries): energy error relative to ground state vs. inverse temperature ( $\beta$ ). Data computed with cubic fragments of size  $l \times l \times l$  spins. Same ten instances at each  $l$ . Dashed lines connect data from same instances.

We first test the solution quality of the algorithm as a function of fragment size: we apply the bootstrapping algorithm to ten instances of  $L = 20$  with cubic fragments of size  $l \times l \times l$  spins with  $l = 3, 4$ , and  $5$ ; with  $l = 6$  we find the computation time of exactly contracting a single fragment to be impractically long. The results are shown in Fig. 3; as expected, the error decreases monotonically with  $l$ , so we use cubic fragments with  $l = 5$  for the rest of the computations.

For  $L = 20, 30, 40$  and  $50$  (ten instances each), the energy error data is shown in Fig. 4, and the time-to-solution (TTS) data is shown in Fig. 5. The minimum error over the tested values of  $\beta$  is  $\lesssim 3\%$ . The error is non-monotonic in  $\beta$  due to finite numerical precision and possibly also finite fragment size. The TTS data closely follows the theoretical expectation of linear scaling.

### B. cubic-lattice tile planting

This model is characterized in Ref. [33]. The model contains multiple base classes of instances, of which we restrict ourselves to the one called  $F_6$ , which is shown in Ref. [33] to be computationally the hardest (i.e., taking the longest time to exactly optimize with Markov-Chain Monte-Carlo methods). Ref. [33] also shows that instances in  $F_6$  are a few orders of magnitude computationally harder than the cubic-lattice  $\pm J$  model. We generate  $F_6$  instances with the Chook library [34]. For all instances, we enable the option in the Chook library to scramble the ground states with gauge transformations.

As with the  $\pm J$  model, we use cubic fragments of size  $5 \times 5 \times 5$  and ten problem instances at each value of  $L$ . The energy error data is shown in Fig. 6, and the TTS data is shown in Fig. 7. The minimum error over the tested values of  $\beta$  at  $L = 50$  is  $\lesssim 5\%$ . The error is non-monotonic in  $\beta$  due to finite numerical precision and possibly also finite fragment

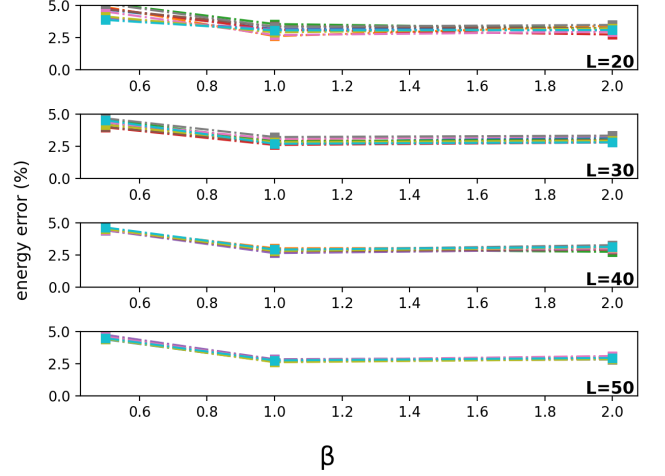


FIG. 4. (color online). Cubic-lattice  $\pm J$  model ( $L \times L \times L$  spins, periodic boundaries): energy error relative to ground state vs. inverse temperature ( $\beta$ ). Data computed with cubic fragments of size  $5 \times 5 \times 5$  spins. Ten instances at each  $L$ . Dashed lines connect data from same instances.

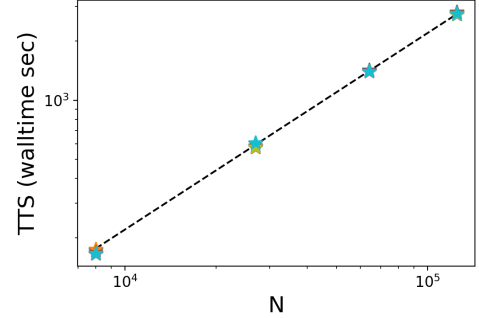


FIG. 5. (color online). Cubic-lattice  $\pm J$  model ( $L \times L \times L$  spins, periodic boundaries): TTS vs. total spins ( $N = L^3$ ) for the simulations of Fig. 4 (ten instances at each  $N$ ). Dashed line denotes theoretically expected linear scaling.

size. The TTS data closely follows the theoretical expectation of linear scaling.

### C. unweighted Max-Cut on random 3-regular graphs

The seminal work of Barahona in Ref. [4] contains a reduction from the problem of unweighted Max-Cut on random 3-regular graphs to the ground-state problem of Eq. (1) on a simple cubic lattice that is only one cube thick with open boundaries and  $J_{ij} \in \{0, \pm 1\}$ . The cubic-lattice model preserves the nonlocal correlations of the original problem by having correlated  $J_{ij}$ . The reduction has a quadratic overhead ( $N = 3V^2$ ) in the number of vertices ( $V$ ) of the random graph. We generate random 3-regular graphs with  $V = 50, 100, 200$ , and  $300$  with the NetworkX library [35], and convert them into cubic-lattice Ising-spin-glass problems via Barahona's reduction. We then apply the bootstrapping algorithm with a fixed

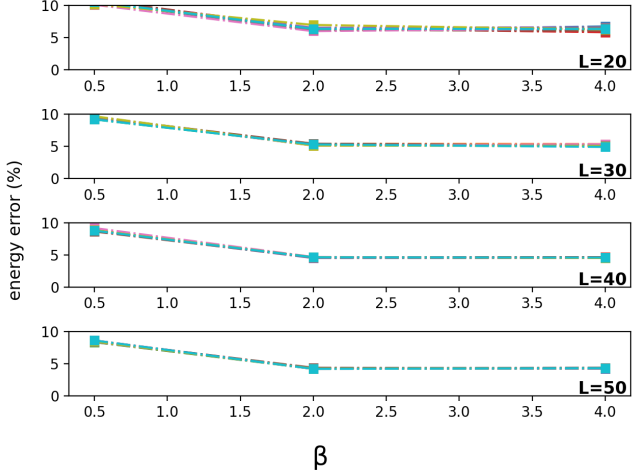


FIG. 6. (color online). Cubic-lattice tile-planting model,  $F_6$  class ( $L \times L \times L$  spins, periodic boundaries): energy error relative to ground state vs. inverse temperature ( $\beta$ ). Data computed with cubic fragments of size  $5 \times 5 \times 5$  spins. Ten instances at each  $L$ . Dashed lines connect data from same instances.

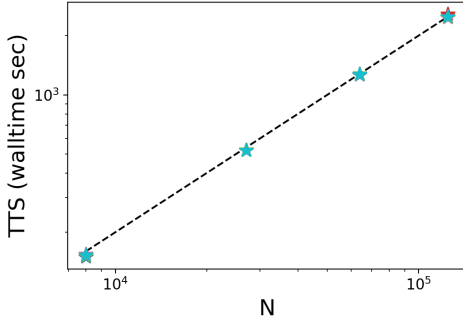


FIG. 7. (color online). Cubic-lattice tile-planting model,  $F_6$  instance class ( $L \times L \times L$  spins, periodic boundaries): TTS vs. total spins ( $N = L^3$ ) for the simulations of Fig. 6 (ten instances at each  $N$ ). Dashed line denotes theoretically expected linear scaling.

fragment size of  $5 \times 5 \times 2$  spins. We compute energy errors by using the exact ground state energies obtained with the McGroundstate server [36]. We use the results in Ref. [4] to compute the approximation ratio from the energies of the low-energy and ground-state spin configurations.

The energy-error, approximation-ratio, and TTS data are shown in Figs. 8, 9, and 10, respectively. The minimum error over the tested values of  $\beta$  is  $\lesssim 1\%$ , and the highest approximation ratio for any given instance is at least about 0.72. The error is non-monotonic in  $\beta$  due to finite numerical precision and possibly also finite fragment size. The TTS data closely follows the theoretical expectation of linear scaling in  $N$ , which translates into a quadratic scaling in  $V$ .

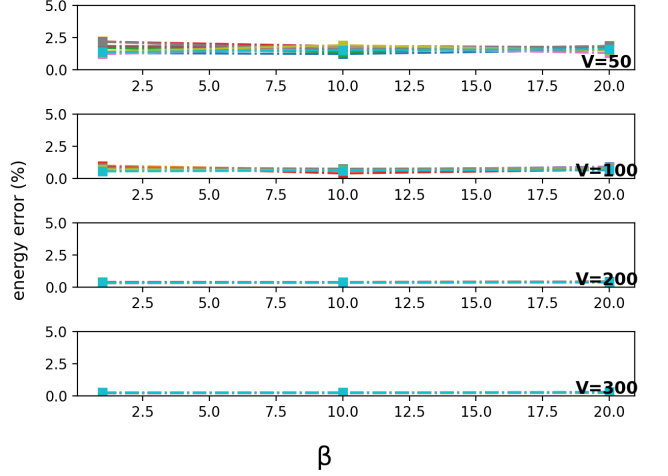


FIG. 8. (color online). Random-3-regular-graph unweighted Max-Cut as a cubic-lattice Ising spin glass: energy error relative to ground state vs. inverse temperature ( $\beta$ ). Data obtained with cubic fragments of size  $5 \times 5 \times 2$  spins. Ten instances at each  $V$  (number of vertices in the random-regular graph). Dashed lines connect data from same instances.

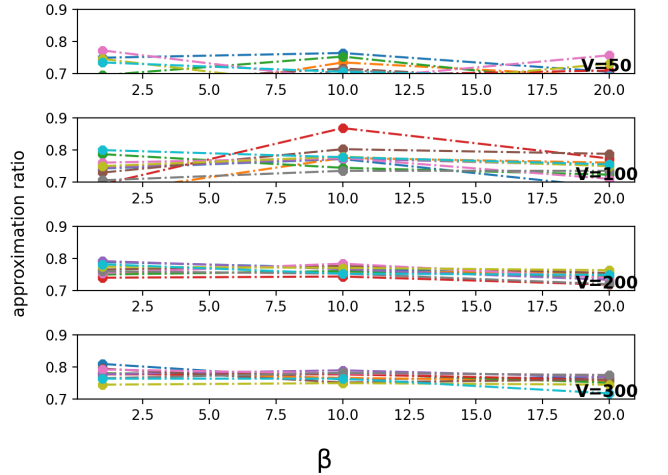


FIG. 9. (color online). Random-3-regular-graph unweighted Max-Cut as a cubic-lattice Ising spin glass: approximation ratio vs. inverse temperature ( $\beta$ ). Data obtained with cubic fragments of size  $5 \times 5 \times 2$  spins. Ten instances at each  $V$  (number of vertices in the random-regular graph). Dashed lines connect data from same instances.

#### IV. THEORETICAL IMPLICATIONS FOR QUANTUM ADVANTAGE

The two sources of error in the present heuristic are finite fragment size and finite  $\beta$ . The latter can be eliminated by switching from regular tensors to tensors that obey tropical algebra [37], which would allow exact ground state computations within each fragment. (Such a maneuver would block implementation of the algorithm on specialized photonic matrix-multiplication hardware, but is useful for the



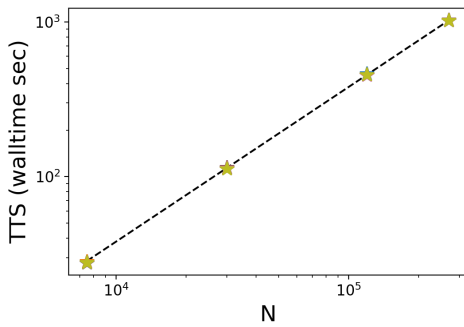


FIG. 10. (color online). random 3-regular-graph unweighted Max-Cut as a cubic-lattice Ising spin glass: TTS vs. total spins ( $N = 3V^2$ ) for simulations of Fig. 8 (ten instances at each  $N$ ). Dashed line denotes theoretically expected linear scaling.

purely theoretical purpose in this section.) We then observe that for spin glasses with both finite-range couplings and finite-range correlations between the couplings, the average energy error of the modified heuristic would monotonically decay with increasing fragment size. Then, an arbitrarily large but fixed fragment size would yield an arbitrarily small average energy error but still result in a linear time complexity. Therefore, the possibility of quantum advantage in the time complexity of heuristic approximate optimization of such spin glasses is not possible for quantum algorithms with linear or superlinear time complexity, regardless of how rugged the energy landscape of such spin glasses may be.

We note, however, that quantum advantage in the time complexity of heuristic approximate optimization is not the only type of possible quantum advantage, even for heuristic quantum algorithms. It remains a possibility, for example, that heuristic quantum algorithms (such as quantum annealing) may exhibit a quantum advantage in obtaining a diverse range of low-energy solutions within some energy error threshold for classical spin glasses, even with linear or superlinear time complexity.

## V. SUMMARY AND DISCUSSION

We have presented and tested a linear-time, tensor-network heuristic for the approximate optimization of cubic-lattice classical spin glasses. The algorithm consists of approximate computations of single-spin marginals at large inverse temperature  $\beta$  via exact contractions of tensor-network fragments; the spins are decimated according to the marginals, and bootstrapping the marginal computations by overlapping the fragments with previously decimated spins yields a global low-energy configuration. We emphasize that the guarantee of linear time complexity comes at the cost of losing any guarantee of solution quality; changing the fragment size, the bootstrapping sequence, the value of  $\beta$ , or the numerical precision can yield different solutions, but there is no guarantee on the error of any of them. We empirically found minimum energy errors relative to the ground state of at most a few percent across three different problem classes of the cubic-lattice classical

Ising model at the largest sizes that we tested.

The first problem class that we tested was the  $\pm J$  model used in recent D-Wave experiments. The quantum annealing D-Wave experiments in Ref. [5] were at a fixed size of over 5,000 spins, and they achieved a minimum energy error of about 2% in a time of about 1  $\mu s$ . The hybrid quantum-classical D-Wave experiments at a size of over 11,000 spins in Ref. [6] achieved a minimum energy error of about 0.1–1% in about one second of total quantum processing time. In comparison, our classical heuristic consistently yielded a minimum energy error of about 3% at sizes 8,000–125,000 spins in a time  $\sim 10^2$ – $10^3$  seconds.

The second problem class that we tested was one with an extremely rugged energy landscape: the  $F_6$  instance class of the cubic-lattice tile planting model. Ref. [33] showed this problem class to have an exact-optimization time a few orders of magnitude larger than the  $\pm J$  model for the leading Monte Carlo heuristics at a system size of  $8 \times 8 \times 8$  spins. Here our heuristic consistently yielded a minimum energy error of about 7% at 8,000 spins and about 5% at 125,000 spins; the error monotonically decreased with system size, suggesting extra error at the system boundaries compared to the bulk. The TTS was the same as with the  $\pm J$  model:  $\sim 10^2$ – $10^3$  seconds.

The third problem class that we tested was the “two-level spin glass” of Barahona [4], which is a local (cubic-lattice) spin glass that encodes the non-local problem of unweighted Max-Cut on random 3-regular graphs. For this problem class our heuristic consistently yielded a minimum energy error of  $\lesssim 1\%$  at system sizes ranging 7,500–270,000 spins, corresponding to random-graph sizes of between 50 and 300 vertices. The approximation ratio was about 0.72–0.88, and the TTS was  $\sim 10^2$ – $10^3$  seconds. The time-complexity of our deterministic heuristic was verified to be quadratic in the number of vertices. In comparison, the well-known Goemans-Williamson approximation algorithm for Max-Cut [38], which often serves as a benchmark for other Max-Cut algorithms, has a guaranteed approximation ratio of  $>0.87856$  and runs in polynomial time.

While the solution quality of our heuristic on the random-3-regular-graph Max-Cut problem does not approach the typical solution quality of the Goemans-Williamson algorithm, it is not very poor either. This seems surprising given that our heuristic operates via a series of *local* approximate optimizations, whereas the problem is intrinsically *nonlocal*. We propose the following explanation: the bootstrapping nature of the algorithm allows the non-local correlations to propagate over the lattice as the spins are successively decimated. It would be interesting in future work to test how well our heuristic works for other local spin-glass problems that encode non-local graph problems. We conjecture that, for fixed fragment sizes, solution quality would decrease with increasing density of the original graph.

On the theoretical side, we explained how the present algorithm implies that quantum advantage in the time complexity of heuristic approximate optimization of classical spin glasses that have decaying correlations is impossible without the candidate quantum algorithm achieving sublinear time complexity, regardless of the ruggedness of the energy landscape of

such spin glasses. This disproves the claim in Ref. [12] of a demonstration of quantum advantage in the time complexity of quantum annealing for heuristic approximate optimization of a short-range spin glass with uncorrelated couplings because the quantum algorithm in Ref. [12] exhibits only superlinear time complexity. This also casts substantial doubt on the belief that short-range classical spin glasses with very rugged energy landscapes are good candidates for demonstrating time-complexity quantum advantage in heuristic approximate optimization.

In industrially-relevant combinatorial optimization problems, what is often desired is a diverse set of low-cost solutions, and some works have therefore addressed the problem of how to sample the low-energy configuration space without bias [39–42]. We expect that our heuristic will not demonstrate good performance in this regard due to the locality of the single-fragment subroutine and also the enhanced sensitivity to finite numerical precision that arises from the exponential form of the Boltzmann weights that are intrinsic to our heuristic. This is consistent with the fact that in none of the tested problem instances was our heuristic able to obtain the ground state. This expectation is also consistent with the findings in the recent work of Ref. [43]. In that work, a branch-and-bound search strategy was combined with tensor-network-contraction marginal computations to approximately optimize quasi-two-dimensional classical spin lattices, and they found that the number of diverse solutions with less than 1% energy error that was generated with that method was a few orders of magnitude less than the number of such solutions obtained with other methods. For future work, therefore, we propose to hybridize the present method with other methods such that the present method is used to efficiently generate a few low-energy solutions that are in turn used as warm starts for other methods that have better performance in terms of exploring the low-energy configuration space, such as the algorithms in Refs. [40, 42].

Another augmentation of the method here could be along the lines of combining it with Monte Carlo similar to what is done in Refs. [29, 44–46]. In those works the sampling bias from approximate tensor-network contractions is corrected with the Metropolis scheme; in the case of the present method the Metropolis scheme could correct the bias that arises from finite fragment sizes.

We are hopeful that such improvements of the present algorithm may provide a new avenue for gaining insights into the properties of classical spin-glass models studied in condensed matter. For example, questions remain open regarding the nature of the low-temperature phase of the cubic-lattice classical  $\pm J$  model [47]. Pure Monte Carlo methods have been the state-of-the-art approach for this problem, but the hybrid methods that we propose would operate according to very different principles and may thereby yield new insights. As another example, Ref. [33] points out that the tunability of the tile-planted-solution model can allow for a systematic study of the interplay between disorder and frustration; the algorithms that we propose may provide a complementary route to pure Monte Carlo methods in such a study as well.

We explained that the algorithm may be parallelized

through simultaneous use of multiple fragments. This would very substantially reduce the simulation time of our heuristic from what is reported here, which would allow the approximate optimization of much larger systems in a practical amount of time. We also noted that one of the sources of error in our implementation of the algorithm, finite temperature, could be eliminated without changing the time complexity: the ordinary tensors could be replaced by tropical tensors [37]. This would likely reduce the energy errors reported in this work at the same fragment sizes, but would not be compatible with adapting the algorithm to specialized photonic hardware in the manner discussed next.

The computational cost of the present heuristic is dominated by matrix multiplications, for which specialized photonic hardware is under active development. Implementation of a heuristic of the present type with such hardware could yield substantially lower time and energy costs. However, it is unlikely that such hardware will be able to achieve beyond about 8 bits of numerical precision in the foreseeable future [48], whereas the results presented here were all with 64 bits of precision. Our (unshown) preliminary tests of our algorithm with `float16` showed very poor results for cubic-lattice tile planting but good results for Barahona’s two-level spin glass. Whether or not the present heuristic can be modified to generally yield sufficiently good warm starts when limited to 8-bit precision is an important open question.

As mentioned, it is possible (and in our opinion very likely) that the heuristic presented in this work will not work well for short-range spin glasses that are reductions or embeddings of dense-graph combinatorial optimization problems. Besides, such optimization problems are more economically represented as dense-graph spin glasses. A tensor-network algorithm that can efficiently optimize dense-graph rugged-energy-landscape spin glasses is therefore desirable. Ref. [49] demonstrates that all-to-all coupled Ising spin glasses can sometimes be optimized by iterating over optimizations of randomly selected subsets of all-to-all coupled spins. In future work we plan to investigate such an approach with the tensor-network machinery that we have demonstrated here, such that the subsets of all-to-all coupled spins take the place of the local fragments in the present algorithm. Our (unshown) preliminary tests on small but very rugged instances of the all-to-all coupled Wishart planted ensemble [50] show good results for approximate optimization without decomposition into subsets. As with the heuristic that we demonstrated in the present work, such a tensor-network approach would be straightforward to generalize to beyond two-body interactions and beyond binary variables.

## ACKNOWLEDGMENTS

We acknowledge discussions with Timothée Leleu, Sam Reifenstein, Victor Bastidas, Wangwei Lan, Johnnie Gray, Yu Tong, Tomislav Begušić, and Garnet Chan. We acknowledge Jack Raymond for pointing out Ref. [32] for the estimated ground state energy of the  $\pm J$  model in the thermodynamic limit.



- 
- [1] D. L. Stein and C. M. Newman, *Spin glasses and complexity*, Vol. 4 (Princeton University Press, 2013).
  - [2] V. Martín-Mayor, J. J. Ruiz-Lorenzo, B. Seoane, and A. P. Young, *Spin glass theory and far beyond: Replica symmetry breaking after 40 years* (World Scientific, 2023) Chap. 5.
  - [3] S. Istrail, Statistical mechanics, three-dimensionality and np-completeness: I. Universality of intracatability for the partition function of the Ising model across non-planar surfaces, in *Proceedings of the thirty-second annual ACM symposium on Theory of computing* (2000) pp. 87–96.
  - [4] F. Barahona, On the computational complexity of Ising spin glass models, *Journal of Physics A: Mathematical and General* **15**, 3241 (1982).
  - [5] A. D. King, J. Raymond, T. Lanting, R. Harris, A. Zucca, F. Altomare, A. J. Berkley, K. Boothby, S. Ejtemaee, C. Enderud, *et al.*, Quantum critical dynamics in a 5,000-qubit programmable spin glass, *Nature* **617**, 61 (2023).
  - [6] J. Raymond, R. Stevanovic, W. Bernoudy, K. Boothby, C. C. McGeoch, A. J. Berkley, P. Farré, J. Pasvolsky, and A. D. King, Hybrid quantum annealing for larger-than-qpu lattice-structured problems, *ACM Transactions on Quantum Computing* **4**, 1 (2023).
  - [7] M. Bernaschi, I. González-Adalid Pemartín, V. Martín-Mayor, and G. Parisi, The quantum transition of the two-dimensional ising spin glass, *Nature* **631**, 749 (2024).
  - [8] R. Ghosh, L. A. Nutricati, N. Feinstein, P. Warburton, and S. Bose, Exponential speed-up of quantum annealing via n-local catalysts, *arXiv preprint arXiv:2409.13029* (2024).
  - [9] By “heuristic approximate optimization” we mean an approximate minimization of the cost function (i.e., Hamiltonian) in a way that lacks a formal guarantee on the error of the minimization.
  - [10] D. Perera, F. Hamze, J. Raymond, M. Weigel, and H. G. Katzgraber, Computational hardness of spin-glass problems with tile-planted solutions, *Physical Review E* **101**, 023316 (2020).
  - [11] G. Jaumà, J. J. García-Ripoll, and M. Pino, Exploring quantum annealing architectures: A spin glass perspective, *Advanced Quantum Technologies* **7**, 2300245 (2024).
  - [12] H. M. Bauza and D. A. Lidar, Scaling advantage in approximate optimization with quantum annealing, *arXiv preprint arXiv:2401.07184* (2024).
  - [13] S. Ciarella, J. Trinquier, M. Weigt, and F. Zamponi, Machine-learning-assisted Monte Carlo fails at sampling computationally hard problems, *Machine Learning: Science and Technology* **4**, 010501 (2023).
  - [14] V. S. Denchev, S. Boixo, S. V. Isakov, N. Ding, R. Babbush, V. Smelyanskiy, J. Martinis, and H. Neven, What is the computational value of finite-range tunneling?, *Physical Review X* **6**, 031015 (2016).
  - [15] A. Perdomo-Ortiz, A. Feldman, A. Ozaeta, S. V. Isakov, Z. Zhu, B. O’Gorman, H. G. Katzgraber, A. Diedrich, H. Neven, J. de Kleer, *et al.*, Readiness of quantum optimization machines for industrial applications, *Physical Review Applied* **12**, 014004 (2019).
  - [16] J. King, S. Yarkoni, J. Raymond, I. Ozfidan, A. D. King, M. M. Nevisi, J. P. Hilton, and C. C. McGeoch, Quantum annealing amid local ruggedness and global frustration, *Journal of the Physical Society of Japan* **88**, 061007 (2019).
  - [17] A. A. Gangat and J. Gray, Hyperoptimized approximate contraction of tensor networks for rugged-energy-landscape spin glasses on periodic square and cubic lattices, *arXiv preprint arXiv:2407.21287* (2024).
  - [18] T. Nishino, Density matrix renormalization group method for 2d classical models, *Journal of the Physical Society of Japan* **64**, 3598 (1995).
  - [19] T. Nishino and K. Okunishi, Product wave function renormalization group, *Journal of the Physical Society of Japan* **64**, 4084 (1995).
  - [20] T. Nishino and K. Okunishi, A density matrix algorithm for 3d classical models, *Journal of the Physical Society of Japan* **67**, 3066 (1998).
  - [21] K. Ueda, R. Otani, Y. Nishio, A. Gendiar, and T. Nishino, Snapshot observation for 2d classical lattice models by corner transfer matrix renormalization group, *Journal of the Physical Society of Japan* **74**, 111 (2005).
  - [22] V. Murg, F. Verstraete, and J. I. Cirac, Efficient evaluation of partition functions of inhomogeneous many-body spin systems, *Physical Review Letters* **95**, 057206 (2005).
  - [23] M. M. Rams, M. Mohseni, D. Eppens, K. Jałowiecki, and B. Gardas, Approximate optimization, sampling, and spin-glass droplet discovery with tensor networks, *Physical Review E* **104**, 025308 (2021).
  - [24] I. Zintchenko, M. B. Hastings, and M. Troyer, From local to global ground states in Ising spin glasses, *Physical Review B* **91**, 024201 (2015).
  - [25] H. Zhou, J. Dong, J. Cheng, W. Dong, C. Huang, Y. Shen, Q. Zhang, M. Gu, C. Qian, H. Chen, *et al.*, Photonic matrix multiplication lights up photonic accelerator and beyond, *Light: Science & Applications* **11**, 30 (2022).
  - [26] S. Ou, A. Sludds, R. Hamerly, K. Zhang, H. Feng, E. Zhong, C. Wang, D. Englund, M. Yu, and Z. Chen, Hypermultiplexed integrated tensor optical processor, *arXiv preprint arXiv:2401.18050* (2024).
  - [27] T. Onodera, M. M. Stein, B. A. Ash, M. M. Sohoni, M. Bosch, R. Yanagimoto, M. Jankowski, T. P. McKenna, T. Wang, G. Shvets, *et al.*, Scaling on-chip photonic neural processors using arbitrarily programmable wave propagation, *arXiv preprint arXiv:2402.17750* (2024).
  - [28] M. H. Latifpour, B. J. Park, Y. Yamamoto, and M.-G. Suh, Hyperspectral in-memory computing with optical frequency combs and programmable optical memories, *Optica* **11**, 932 (2024).
  - [29] T. Chen, E. Guo, W. Zhang, P. Zhang, and Y. Deng, Tensor network Monte Carlo simulations for the two-dimensional random-bond Ising model, *arXiv preprint arXiv:2409.06538* (2024).
  - [30] J. Gray, quimb: A python package for quantum information and many-body calculations, *Journal of Open Source Software* **3**, 819 (2018).
  - [31] J. Gray and S. Kourtis, Hyper-optimized tensor network contraction, *Quantum* **5**, 410 (2021).
  - [32] U. Gropengiesser, The ground-state energy of the  $\pm J$  spin glass. A comparison of various biologically motivated algorithms, *Journal of Statistical Physics* **79**, 1005 (1995).
  - [33] F. Hamze, D. C. Jacob, A. J. Ochoa, D. Perera, W. Wang, and H. G. Katzgraber, From near to eternity: spin-glass planting, tiling puzzles, and constraint-satisfaction problems, *Physical Review E* **97**, 043303 (2018).
  - [34] D. Perera, I. Akpabio, F. Hamze, S. Mandra, N. Rose, M. Aramon, and H. G. Katzgraber, Chook—a comprehensive suite for generating binary optimization problems with planted solutions, *arXiv preprint arXiv:2005.14344* (2020).

- [35] A. Hagberg, P. J. Swart, and D. A. Schult, *Exploring network structure, dynamics, and function using NetworkX*, Tech. Rep. (Los Alamos National Laboratory (LANL), Los Alamos, NM (United States), 2008).
- [36] J. Charfreitag, M. Jünger, S. Mallach, and P. Mutzel, Mc-Sparse: Exact solutions of sparse maximum cut and sparse unconstrained binary quadratic optimization problems, in *2022 Proceedings of the Symposium on Algorithm Engineering and Experiments (ALENEX)*, edited by C. A. Phillips and B. Speckmann (2022) pp. 54–66.
- [37] J.-G. Liu, L. Wang, and P. Zhang, Tropical tensor network for ground states of spin glasses, *Physical Review Letters* **126**, 090506 (2021).
- [38] M. X. Goemans and D. P. Williamson, . 879-approximation algorithms for max cut and max 2sat, in *Proceedings of the twenty-sixth annual ACM symposium on Theory of computing* (1994) pp. 422–431.
- [39] Z. Zhu, A. J. Ochoa, and H. G. Katzgraber, Fair sampling of ground-state configurations of binary optimization problems, *Physical Review E* **99**, 063314 (2019).
- [40] E. Ng, T. Onodera, S. Kako, P. L. McMahon, H. Mabuchi, and Y. Yamamoto, Efficient sampling of ground and low-energy Ising spin configurations with a coherent Ising machine, *Physical Review Research* **4**, 013009 (2022).
- [41] M. Mohseni, M. M. Rams, S. V. Isakov, D. Eppens, S. Pielawa, J. Strumpfer, S. Boixo, and H. Neven, Sampling diverse near-optimal solutions via algorithmic quantum annealing, *Physical Review E* **108**, 065303 (2023).
- [42] T. Leleu and S. Reifenstein, Non-equilibrium dynamics of hybrid continuous-discrete ground-state sampling, arXiv preprint arXiv:2410.22625 (2024).
- [43] A. M. Dziubyna, T. Śmierzchalski, B. Gardas, M. M. Rams, and M. Mohseni, Limitations of tensor network approaches for optimization and sampling: A comparison against quantum and classical Ising machines, arXiv preprint arXiv:2411.16431 (2024).
- [44] A. J. Ferris, Unbiased monte carlo for the age of tensor networks, arXiv preprint arXiv:1507.00767 (2015).
- [45] W. Huggins, C. D. Freeman, M. Stoudenmire, N. M. Tubman, and K. B. Whaley, Monte Carlo tensor network renormalization, arXiv preprint arXiv:1710.03757 (2017).
- [46] M. Frías Pérez, M. Mariën, D. Pérez García, M. C. Bañuls, and S. Iblisdir, Collective Monte Carlo updates through tensor network renormalization, *SciPost Physics* **14**, 123 (2023).
- [47] S. Caracciolo, A. Hartmann, S. Kirkpatrick, and M. Weigel, Spin glass theory and far beyond: Replica symmetry breaking after 40 years (World Scientific, 2023) Chap. 1.
- [48] R. Hamerly, (private communication).
- [49] H. Cilasun, Z. Zeng, A. Kumar, H. Lo, W. Cho, W. Moy, C. H. Kim, U. R. Karpuzcu, and S. S. Sapatnekar, 3sat on an all-to-all-connected cmos ising solver chip, *Scientific reports* **14**, 10757 (2024).
- [50] F. Hamze, J. Raymond, C. A. Pattison, K. Biswas, and H. G. Katzgraber, Wishart planted ensemble: A tunably rugged pairwise ising model with a first-order phase transition, *Physical Review E* **101**, 052102 (2020).